Soft Matter

Mix and Match — a Versatile Equilibrium Approach for Hybrid Colloidal Synthesis

Journal:	*Soft Matter*
Manuscript ID	SM-COM-02-2020-000202.R1
Article Type:	Communication
Date Submitted by the Author:	20-Apr-2020
Complete List of Authors:	Ben Zion, Matan Yah; New York University, Physics; ESPCI Paris, Gulliver Caba, Yaelin; New York University, Physics Sha, Ruojie; New York University, Department of Chemistry Seeman, Nadrian; New York University, Department of Chemistry Chaikin, Paul; New York University, Physics

Mix and Match — a Versatile Equilibrium Approach for Hybrid Colloidal Synthesis

Matan Yah Ben Zion[*†‡], Yaelin Caba[†], Ruojie Sha[§], Nadrian C. Seeman[§], Paul M. Chaikin[†]*

† Center for Soft Matter Research, Department of Physics, New York University, 726 Broadway, New York, NY 10003, United States

§ Chemistry Department New York University, 24 Waverly Pl., New York, NY, 10003, USA

colloids; self-assembly; nano-particles; DNA; metamaterials

Colloidal synthesis is a powerful bottom-up approach for programmed self-assembly which holds promise for both research and industry. While diverse, each synthetic process is typically restricted to a specific chemistry. Many applications however require composite materials, whereas a chemical equilibrium can typically only match one material but not the other. Here, a scalable general approach is presented, alleviating the dependency on a specific chemical reaction, by resorting to a mechanical equilibrium; an isopycnic density-gradient-step is tailored to form clusters with prescribed composition. Valence control is demonstrated, making dimers, trimers, and tetramers with purity as high as 96%. The measured kinetics shows a scaleable throughput. The density gradient step plays a dual role of both filtering out undesired products and concentrating the target structures. The "Mix-and-Match" approach is general, and applies to a broad range of colloidal matter: diverse material compositions (plastics, glasses, and emulsions); a range of colloidal interactions (van-der-Waals, Coulomb, and DNA hybridization); and a spectrum of sizes (nanoscale to multiple micrometers). Finally, the strength of the method is displayed by producing a monodisperse suspension from a highly polydisperse emulsion. The ability to combine colloids into architectures of hybrid materials has applications in pharmaceuticals, cosmetics, and photonics.

The past decades have seen a renaissance of nano and micro particle synthesis.[1-18] Development in fabrication at the mesoscale extended the repertoire of such constructs to include a variety of materials and particle interactions (vdW, Coulomb, and DNA),[15] tunable optical response, and predesigned geometries. This palette provides a route to unprecedented bottom up control of self assembly on the micron scale. Today, a diverse range of nano and micron size particles are also commercially available, or can be synthesized with minimal effort. This makes particles of a specific size and material readily accessible for physicists, chemists, and biologists. Many applications however require a combination of material properties not found in a single type of colloid: the optical response of a single nano particle can be finely tuned[19] but will require attachment to a bulkier micron size colloid for the periodic assembly of a photonic crystal with tunable disorder[20-23]; a micro fluidic droplet can dissolve a drug molecule, but may require a magnetic particle to serve as a vehicle for its targeted delivery.[24] For these, and other practical purposes, a general approach of forming hybrid clusters is desirable. In order to address this need we adopt a technique common in biology – density gradient centrifugation. Originally developed to elucidate the molecular nature of living matter,[25] density centrifugation is now widespread in biochemistry, and medicine,[26, 27] and accessible in many laboratories. In this work, we show that when modified, density centrifugation can be transformed from an analytic method to a powerful synthetic strategy.

As a first example of this approach, we demonstrate the making of colloidal dimers by mixing two suspensions of oppositely charged particles. Positive and negative particles spontaneously bind, and if allowed to proceed indefinitely, will aggregate into macroscopic clumps. To prevent their aggregation, the reaction is halted at an early stage, but still contains trimers and higher clusters. By using particles with different specific gravities, it is possible to density match the fluid to the density of a dimer. **Figure 1** illustrates an example of such a process: 2μL of positively charged silica particles (1.86μm, 1%v/v, Bangs Lab) are mixed with 10 μL negatively charged polystyrene (PS) particles (4.2 μm, 1%v/v, Bangs Lab) in a 1.5 mL micro-centrifuge tube with 88 μL of 11 mM sodium chloride solution. The reaction is quenched after 10 seconds by a ten-fold dilution using a Pluoronic solution (F-127 0.5%w/w). The density of the target silica-PS dimers is simply given by a weighted sum

$$\rho_{dimer} = \frac{m_{silica} + m_{PS}}{V_{silica} + V_{PS}} = \frac{\rho_{silica} r_{silica}^3 + \rho_{PS} r_{PS}^3}{r_{silica}^3 + r_{PS}^3} = 1.126 g/cc, \tag{1}$$

where r_x is the radius of particle x ($2r_{PS}$ = 4.2 μm, $2r_{silica}$ = 1.86 μm) and ρ_x is its density (ρ_{PS} = 1.05g/cc, ρ_{silica} = 2.0g/cc). The equilibrium density separation follows by using a density notch filter: a centrifuge tube (SETON SCIENTIFIC 7030) is layered with three fluids of different densities (see Figure 1a) — A high density sucrose solution (1.135 g/cc), an intermediate density sucrose solution (1.062 g/cc) and the reaction solution which is water based (0.998 g/cc). The layered tube is then loaded to a swinging bucket centrifuge (Thermo Scientific IEC Multi RF Refrigerated Centrifuge). When centrifuged, the dimers accumulate at the sucrose-sucrose interface and form a visible band that can be readily extracted with a syringe and a needle (BD

Precision Glide Needle 27GX1/2). Inspection with an optical microscope[28] suggests a purity of 96%, a yield of 10% (with PS being the limiting reagent) and a through-put of 0.2 mg dimers (9 million particles) per 1 mL reaction solution per minute reaction time (see Figure 1c-d, table I). The dimers are stable and can be concentrated to high volume fraction and stored for months.

We find that the mass distribution matches the dimers' design by measuring their fluctuating orientation. Figure 1b, shows a side view of the dimers taken on a tilted microscope (gravity pointing down, see Supporting Movie 1). The probability distribution $P(\theta)$ of 37,000 different captured orientations, θ, relative to the vertical is then extracted. On average, the dimers are pointing downwards with the denser silica particle at the bottom, but thermal fluctuations allow each dimer to explore other angles. The probability distribution at the small angle approximation of finding a dimer at a given angle is

$$P(\theta) = P(0)exp\left(-\frac{1\mu gL}{2k_BT}\theta^2\right), \qquad (2)$$

where μ is the reduced mass, L is the length of the dimer, k_B is the Boltzmann factor, and T is the absolute temperature, (see Methods for full derivation). By fitting the measured potential energy (blue dots) to a harmonic potential (red curve), the measured reduced mass $\mu_{measured} = 1.20 \pm 0.09$ pg is in excellent agreement with the design $\mu_{designed} = 1.28$ pg with no fitting parameters.

Other synthetic methods that use centrifugation as a key step scale poorly as they do not use an equilibrium property.[1,5,29,30] Instead they rely on the different mobility of the target structure, making the process much slower (days instead of minutes) and very sensitive to the separation protocol, requiring careful tuning to separate product bands of minute mobility differences. The gradient-step approach described here, scales well and is robust to the details of the protocol for two reasons: 1) the target structures accumulate at their equilibrium gravitational position as prescribed by the density step interface. For a given centrifugal force *a,* and tube length *L*, the band's position is insensitive to the centrifugation duration above a minimal time T_{min}, which in our example is about 1 min, estimated using $T_{min} = \frac{\xi L}{ma}$, where ξ is the drag coefficient of the particle, and m is the buoyant mass. Experimenting with different centrifugation conditions we find the process to work for centrifugation duration between 5 minutes and 2 hours and centrifugation rates between 1-3.5kRCF. We chose to work with higher centrifugal accelerations to reduce process duration and avoid density-gradient diffusive smearing. 2) the target structure is not stressed when concentrated as particles accumulate at a fluid-fluid interface. They do not experience the sort of destabilizing stress which is present on a solid surface. This allows a higher centrifugal force, and a quicker, more efficient process.

The Mix and Match method extends beyond dimers to higher clusters such as trimers and tetramers. **Figure 2** demonstrates the production of clusters with controlled valency from commercially available magnetic particles, (dynabeads, Bangs Lab M280) and homemade nC14 oil-emulsion (n-Tetradecane stabilized with SPAN-80, see Methods for protocol). To target a specific cluster, the sucrose density steps were tuned (1.09/1.11 g/cc for dimers; 1.07/1.09 g/cc for trimers; and 1.05/1.07 g/cc for tetramers). The values were chosen based on a modified version of Equation 1 which accounts for a multiple number of satellite emulsion particles, N_e:

$$\rho = \frac{N_e m_e + m_m}{N_e V_e + V_m} = \frac{N_e \rho_e r_e^3 + \rho_m r_m^3}{N_e r_e^3 + r_m^3}, \qquad (3)$$

where the subscript X_m (X_e) refers to the magnetic bead (emulsion). To increase the number of satellite particles further, the reaction between the magnetic beads and the emulsion was allowed to proceed for 5 minutes (longer than in the case of the dimers). Naturally, purity, yield, and throughput decrease with an increase in the complexity of the structure (number of satellite particles), predominantly due to the polydispersity of the reacting colloids (M280 has a polydispersity index of 5% as received, and the polydispersity of the nC14 emulsion is 10%).

When a structure with a specific valency, rather than a specific shape is sought,[5, 31-35] we found that it is possible to optimize the purification of clusters with N satellites by setting ratio between the radius of a satellite particle *r* and the radius of the central particle *R*:

$$\frac{r}{R} = \frac{1}{\sqrt[6]{N(N+1)}}. \qquad (4)$$

The functional dependence of this 'magic ratio' is illustrated in Figure 2f (see Methods for a full derivation). The ratio in Equation 4 maximizes the density difference between the target cluster with N satellite particles, and the cluster of closest density, of N + 1 satellite particles. Note that the ratio only requires the densities to be different and does not depend on their explicit value.

Synthetic methods for making colloidal and nanoparticle structures can rely on different binding forces with varying specificity most notably including — wetting and van der Waals, Coulomb attraction,[36, 37] and DNA hybridization.[12, 17, 38] The Mix-and-Match approach is general and applies to a myriad of particle-particle interactions. **Figure 3a-c** shows clusters formed by different binding forces: van der Waals binding (Figure 3a), Coulomb attraction (Figure 3b), and binding with DNA origami (Figure 3c). DNA origami functionalized colloids were shown to make very rich clusters from nanoparticles to the colloidal scale, controlling geometry and chirality, and in conjunction with equilibrium density matching can form pure samples of the target structure.[39] Figure 3c shows that this method is also applicable to submicron particles, and can be further extended to the quickly growing inventory of DNA coated nano particles and quantum dots.[15, 17, 38, 40-43]

The kinetic rate and throughput of the process were measured by tracking the progress of the reaction using 3 μm magnetic beads (M280 Bangs Lab), and a homemade 3 μm n-Decane emulsion (nC10). Both particles are negatively charged and bind nonspecifically through vdW interaction once they overcome their screened Coulomb repulsion. The reaction proceeds by mixing an equimolar ratio ($\varphi = 0.1\%$) of the magnetic particles and the droplets in 450 μL deionized water. The suspension is then destabilized by adding 50 μL of 0.1 M sodium chloride solution which lowers the Debye screening length to a few nanometers, initiating the reaction. The reaction is quenched after a predefined intervals by a ten fold dilution. The maximal quench time can be estimated by the average first arrival time assuming a diffusion limited reaction and using Smoluchowski's result[44]

$$\tau = \frac{1}{4\pi r n D} \approx 15 min, \qquad (5)$$

where we have used the reactant concentration $n \approx 2.5\cdot10^{-4}/\mu m^3$, target radius $r \approx 1.5$ μm, and the reactant-target pair diffusion constant $D \approx 0.24$ $\mu m^2/s$. With this assumption, we can systematically monitor the reaction progression.

After initiation, we measured the progress of the reaction by monitoring the levels of unreacted particles at increasing time intervals between 0−10 min. At each interval, a 2 μL aliquot was extracted from the reaction pot and immediately quenched. The number of unreacted magnetic beads was counted using an optical microscope, and their reactivity estimated accordingly. The reaction rate of the magnetic particles of concentration n with the oil droplets of concentration m can be written as $\frac{dn}{dt} = -Kmn$. Given the similarity in size and concentration for both the targets and the reactants $m \approx n$, and without loss of generality, the above equation simplifies to $\frac{dn}{dt} = -K n^2$, of which solution is

$$\frac{1}{n(t)} = \frac{1}{n_0} + Kt, \tag{6}$$

where n_0 is the initial concentration, and K is the reaction rate constant. Figure 2e shows a linear fit to Equation 6 with a slope of $p = 8.9 \cdot 10^{-6} s^{-1}$. The average first arrival time is therefore $\tau = \frac{1}{pN_0} = 17min$, within 12% of the original estimate. From this kinetic analysis we can compute the kinetic rate constant of the process: $3 \cdot 10^6 \frac{particles}{min \cdot mL}$. The final throughput is further reduced by approximately a factor of three due to parasitic processes (such as sticking to reaction tube walls and losses in the separation process). Our experience shows that with increasing volume there is also an increase in throughput. The measured throughput, purity and yield for the different types of interactions are summarized in **Table 1**. Serial processes, such as microfluidics can also produce diverse colloidal clusters[45] but have a lower throughput (less than $3 \cdot 10^3 \frac{particles}{min}$), and cannot be simply scaled by volume.

Finally, we show that the Mix-and-Match approach can produce a monodisperse product even from a highly polydisperse reactants. We prepared a polydisperse emulsion by sonicating n-Tetradecane in water (see Methods for protocol) with droplets' diameters spanning three orders of magnitude (0.4 – 400 µm). This highly polydisperse suspension is then mixed with commercial M280 dynabeads and allowed to react for one minute (Figure 3d). Once reacted, clusters with a wide variety of sizes and constituents were formed. We designed a density gradient step to match equisized dimers. Upon density step separation, a suspension of 71% dimers is extracted. The oil droplets in the dimers are highly uniform in size with a standard deviation smaller than 10%.

In this work we have described a general technique for synthesis and purification of hybrid colloidal constructs that is applicable on the nano and micro scales. The technique relies on a tunable mechanical equilibrium rather than a specific chemical process. We have shown that this method can produce predesigned dimers from commercially available suspensions with high purity (higher than 95%), as well as trimers and tetramers, and in principle any cluster limited only by the density matching precision. Purity can also be further increased by simply repeating the process. The approach was demonstrated to apply to a range of commercially available particles of a variety of materials (polymers, glass, and oils), applicable for a range of colloidal interactions (van der Waals, Coulomb, and DNA hybridization), and suitable for both solid and fluid particles. The method can also be adapted to non spherical particles. Being general, this approach will prove useful in rapid production of future functional materials.

Methods

Experimental Methods

Sonication Emulsification Synthesis

In a micro-centrifuge tube n-Tetradecane 0.4mL with 0.1%w/w SPAN 80 and 0.6mL water were mixed by first vortexing and then sonicating in a sonication bath for 5min.

Membrane Emulsification Synthesis

Oil in water emulsions were synthesized using membrane emulsification with a typical droplet size was 3.0 ± 0.6 μm (see **Figure S1**). For this, SPAN80 (Sigma Aldrich) was pre-dissolved in a linear saturated alkane oil (the procedure works for alkanes ranging from octane to hexadecane). 10 mL of oil were loaded into the emulsification cup with a 0.5 μm membrane (SPG technology) dipped in 100 mL deionized water. While stirring with a magnetic stirrer, the oil is over pressurized to 100 − 200kPa, resulting in formation of an oil in water emulsion. Once complete, the emulsion in transferred to a separation funnel to improve monodispersity. Stock suspensions are stable for at least six months at room temperature.

Colloid DNA-functionalization

The DNA sticky ends were attached to the colloids by click chemistry through the azide terminated polymer brush. For this a PS-b-PEO diblcock copolymer hydroxyl end was reacted with sodium azide (NaN_3) using methanesulphonylchloride (99.7% Sigma Aldrich). The full procedure is found in Ref. 39. Colloids were then coated with the azide terminated di-block and dyed in a single swelling-deswelling step. A 50μL colloidal suspension (Bangs Lab, 10% volume fraction in water, as received, see list of colloids in materials) was swelled in 400 μL 70%-

30%v/v DI H_2O-Tetrahedrofuoran and 3 μL BODIPY based dye, by agitation for 30 mins. Dyed colloids were visible on the fluorescence microscope after 5mins. 1mL of deionized water added for the deswelling and the THF was allowed to evaporate (30 mins on a 50^{o}C plate or 2h at room temperature) with occasional shaking. Suspensions were washed 4 times by centrifuging and decanting with DI water to a final volume of 1 mL and 0.5% volume fraction. Finally the azide terminated polymer brush on the colloidal particles was reacted with 5' end functionalized dibenzenecyclooctane (DBCO) DNA sticky ends (see list in materials).

Optical microscope sample preparation

Samples were pipette loaded into pre treated capillaries. Capillaries (0.10mm 2.00mm internal dimensions, Vitrotubes W5010-050) were pre-cleaned for 30min with O_2 plasma (SPI supplies Plasma Prep II) and coated with hexamethyldisilazane (HMDS) through vapor deposition by leaving them in a sealed petri dish with a 0.1mL HDMS over night. After sample loading, the capillaries were sealed with UV curable resin (LOON OUTDOORS UV CLEAR FLY FIN- ISH) cured with a UV flashlight.

Scanning Electron Microscope Sample Preparation

The suspension of the negatively charged DNA colloidal clusters was deposited onto a positively charged silicon wafer. A pre-scribed 5 mm X 5 mm, 100 nm oxide silicon wafer was sonication cleaned in the following baths: acetone, isopropyl alcohol, and deionized water then nitrogen dried, and plasma cleaned for 15 minutes. The clean wafer is dipped for 5 minutes in a 1% PDADMAC solution in 2M NaCl, then transferred to a deionized bath for another 5 minutes (for salt removal), and then nitrogen dried. The colloidal suspension (0.01%v/v) is then directly deposited onto the dried wafer, allowing 5 minutes for particles to sediment and stick to the oppositely charged wafer surface, and finally nitrogen dried. The colloids can then be directly imaged using secondary electron emission, with or without 2 nm gold sputtering.

Instrumentation

Scanning Electron Microscope images were acquired using a Carl Zeiss MERLIN Field Emission Scanning Electron Microscope. Optical microscopy was performed using a Leica DMRX Optical Microscope and a home made tilted microscope for the dimers side view experiments.

Materials

Colloids

The following colloidal suspensions were purchased from Bangs Lab:

M280 particles (Bangs Lab), 0.69 µm and 4.2 µm polystyrene particles, amine terminated 1.86 µm silica particles, and 0.7 µm PMMA particles.

DNA

DBCO Modified DNA oligos strands were purchased from (IDT DNA):

For coating for coating PS 0.69µm: /5DBCON/$(T)_{20}$GTATTCGAGTT, and /5DBCON/(T)20GATGGATTAGG. PMMA 0.71µm coating: /5DBCON/$(T)_{20}$CTCAATAC.

Dye molecules

Powder BODIPY based dyes were purchased from Thermofisher and dissolved in toluene to make a 1mg / mL solution:

BODIPY-FL BODIPY FL NHS Ester (Succinimidyl Ester) D-2184 503/512.

BODIPY-650/665 BODIPY 630/650-X NHS Ester (Succinimidyl Ester) D-10000 646/660

Reagents

n-Decane, n-dodecane, n-Tetradecane and n-Hexadecane, SPAN 80, poly diallyl dimethyl ammonium chloride (PDADMAC) MW = 450 kDa, hexamethyldisilazane (HMDS), methanesulphonylchloride (99.7%), sodium azide (NaN_3), toluene, tetrahydrofuran (THF) were purchased from Sigma Aldrich. PEO diblock copolymer (P10078A-SEO, PS-b-PEO 3.8kDa,6.5kDa), was purchased from Polymer Source. Pluoronic F-127 from BASF.

Theoretical Methods

Measuring Mass Distribution From Dimer Orientation

The potential energy of two masses m_1 and m_2 in a gravitational potential is:

$$U_{tot} = m_1 g y_1 + m_2 g y_2 \qquad \text{(S1)}$$

The position of each mass can be expressed as its distance from the masses' center of mass (CoM) $y_i = y_{cm} + \Delta y_i$, which makes **Equation S1** $U_{tot} = Mgy_{CoM} + m_1 g\Delta y_1 + m_2 g\Delta y_2$, where $M = m_1 + m_2$ is the total mass. This allows us to separate the potential energy into the center of mass energy $U_{CoM} = M\, g\, y_{CoM}$ the contribution of the two masses' orientation to the potential energy, $U_{or} = m_1 g\Delta y_1 + m_2 g\Delta y_2$. Given that each mass is a sphere of radius r_i, its center distance from the CoM is $r_i = (1-m_i/M)(r_1+r_2)$. As the masses are rigidly connected, the vertical separation from the CoM is simply given by, $\Delta y_i = \Delta r_i \cos\theta$ (see **Figure S2**). Defining the reduced mass $\mu \equiv$

$m_1 \cdot m_2/(m_1+m_2)$, and the dimer length $L \equiv d_1 + d_2 = 2(r_1 + r_2)$ where d_i is the diameter of a particle, results in the following orientational potential energy for a dimer given in the main text

$$U_{or} = \mu\, g\, L \cos\theta \qquad \text{(S2)}$$

Assuming small displacements, $\theta \ll 1$, we can expand the alignment energy of the simple pendulum (**Equation S2**) to result in the potential energy of a mathematical pendulum $U_{or} \approx \mu g L(1-0.5\theta^2)$. Using the Boltzmann distribution to express the probability P of finding the dimer aligned at an angle θ one finds $P(\theta) = P(0)exp\left(-\frac{1}{2}\Gamma\theta^2\right)$, where $\Gamma \equiv \mu\, g\, L / k_B T$ (Equation 2 in the main text). Figure 1c gives the measured probability distribution measured of over 37,000 different angles θ. Taking the logarithm of the distribution and fitting to a parabola for small angles, gives the oscillator strength of the pendulum: $\Gamma = 17.30 \pm 0.10$. We can then extract the reduced mass by using the particles' diameters $d_{PS} = 4.2$ μm, $d_{silica} = 1.86$ μm, gravitational acceleration $g = -9.8$ m/s^2, and absolute room temperature $T = 298$K, finding: $\mu_{measured} = 1.20 \pm 0.09$ pg. Using the material densities of the two particles, $\rho_{PS} = 1.05$ g/cc, $\rho_{silica} = 2.0$ g/cc, we can compute the designed reduced mass, $\mu_{designed} = 1.28$ pg, in quantitative agreement with the measurement.

Magic Ratio Derivation

We look for the optimal radii ratio between satellite particles r and center particle R, with densities ρ_r and ρ_R respectively, in a target cluster with N satellite particles. Rewriting Equation 3 from the main text in dimensionless fashion gives

$$\rho = \rho_R \frac{N\grave{\rho}x + 1}{Nx + 1}, \qquad \text{(S3)}$$

where we define $x \equiv \left({}^{r}/_{R}\right)^{3}$, and $\grave{\rho} \equiv {}^{\rho_r}/_{\rho_R}$. Differentiation **Equation S3** by x gives $\frac{\partial \rho}{\partial x} = \frac{N}{(Nx+1)^2}$ $\rho_R(\grave{\rho}-1)$. Assuming that the impurity that is hardest to separate by density is that of clusters with *N+1* satellite particles, we can define the densities difference, Δ as $\Delta(N) \equiv \rho(N)-\rho(N+1)$, with an extremum given by

$$\frac{\partial \Delta}{\partial x} = 0 = \rho_R(\grave{\rho}-1)\left[\frac{N}{(Nx+1)^2}-\frac{N+1}{((N+1)x+1)^2}\right]. \qquad \text{(S4)}$$

From **Equation S4** it is apparent that there is no extremum when the densities are equal ($\grave{\rho} = 1$), and that the position of the extremum does not depend on the densities. This equations solves when $x = [(N+1)N]^{-0.5}$ which gives radii ratio (Equation 4 in the main text).

Reaction Rate Derivation

From Smoluchowski,[44] the first arrival time, τ, of particles N to target M is given as the inverse of the reaction rate *k*, $\tau^{-1} = k = 4\pi BDn$, where B is the target size, D is the diffusion constant of particles *N*, and *n* is their number concentration $n \equiv {}^{N}/_{V}$ where V is the volume. The total number of reacting particles per unit time $dN/dt = -k \cdot M$, and *M* the number of targets. Dividing by the volume *V*, we find $dn/dt = -k \cdot m = -4\pi BDn \cdot m$. In our system, N and M are treated symmetrically (same size and concentration), therefor we can identify $n \approx m$ to give the kinetic equation $dn/dt = -4\pi BDn^2$, which solves to $1/n - 1/n_0 = 4\pi BD\, t$ (Equation 6 in the main text), where n_0 is the initial concentration. The concentration after the quench, n_q is reduced by a factor *q,* $n = q \cdot n_q$. Given the volume of the microscope's field of view (FOV) V_{FOV}, the observed number of particles within the FOV is then given by $N_q = n_q \cdot V_{FOV}$ finally gives, the linear depends that is fitted in Figure 2e in the main text to extract the kinetic parameters $\frac{1}{N_q(t)}-\frac{1}{N_q(0)}x$ $= 4\pi BD\frac{q}{V_{FOV}} \times t$.

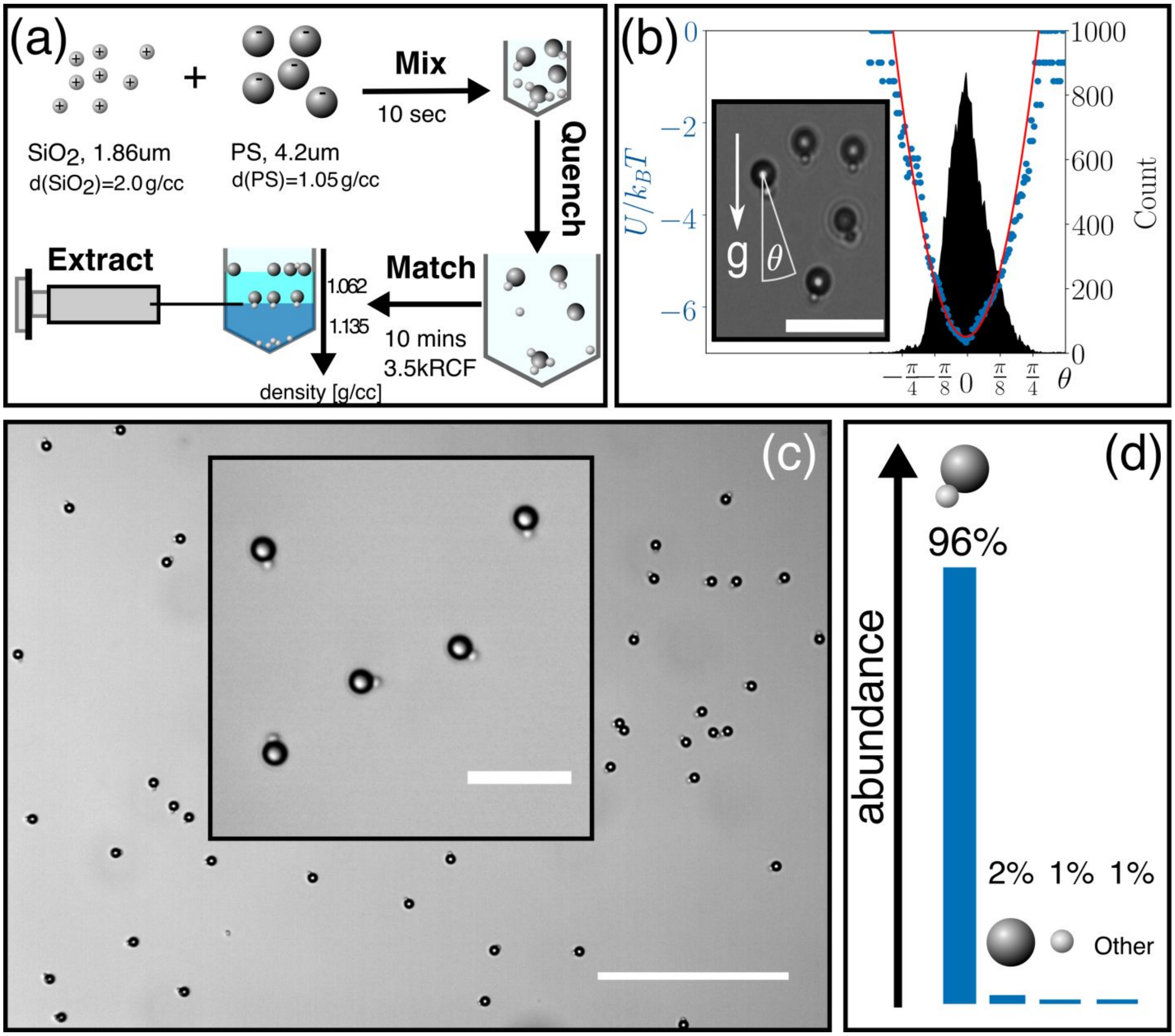

Figure 1. Dimer formation using Mix-and-Match approach to get 96% purity dimers. a) Steps of the Mix-and-Match approach: *i* positively charged 1.86 μm silica particles are mixed with negatively charged 4.2 μm polystyrene particles and start to spontaneously react. *ii* The reaction is quenched by dilution, preventing formation of large aggregates. *iii* The target silica-PS dimers are extracted by matching a tailored density gradient step. b) Probability distribution (black) of finding a dimer at angle θ off the vertical when observed from the side. Using the Boltzmann distribution (Equation 2), the potential energy can be computed $U_{or}(\theta)$, (blue dots) and fitted to a

harmonic potential (red curve). Inset shows the dimers as seen from the side on a tilted microscope with gravity pointing downwards. See Figure S2 and Supporting Movie 1. c) A typical field of view after separation showing only hybrid silica-PS dimers. c) Cluster abundance as counted from over 300 clusters (all observed particles are accounted for including singlets). The dimers are stable and can be stored for months. scalebars: b: inset 20 µm. c: 100 µm (inset, 20 µm).

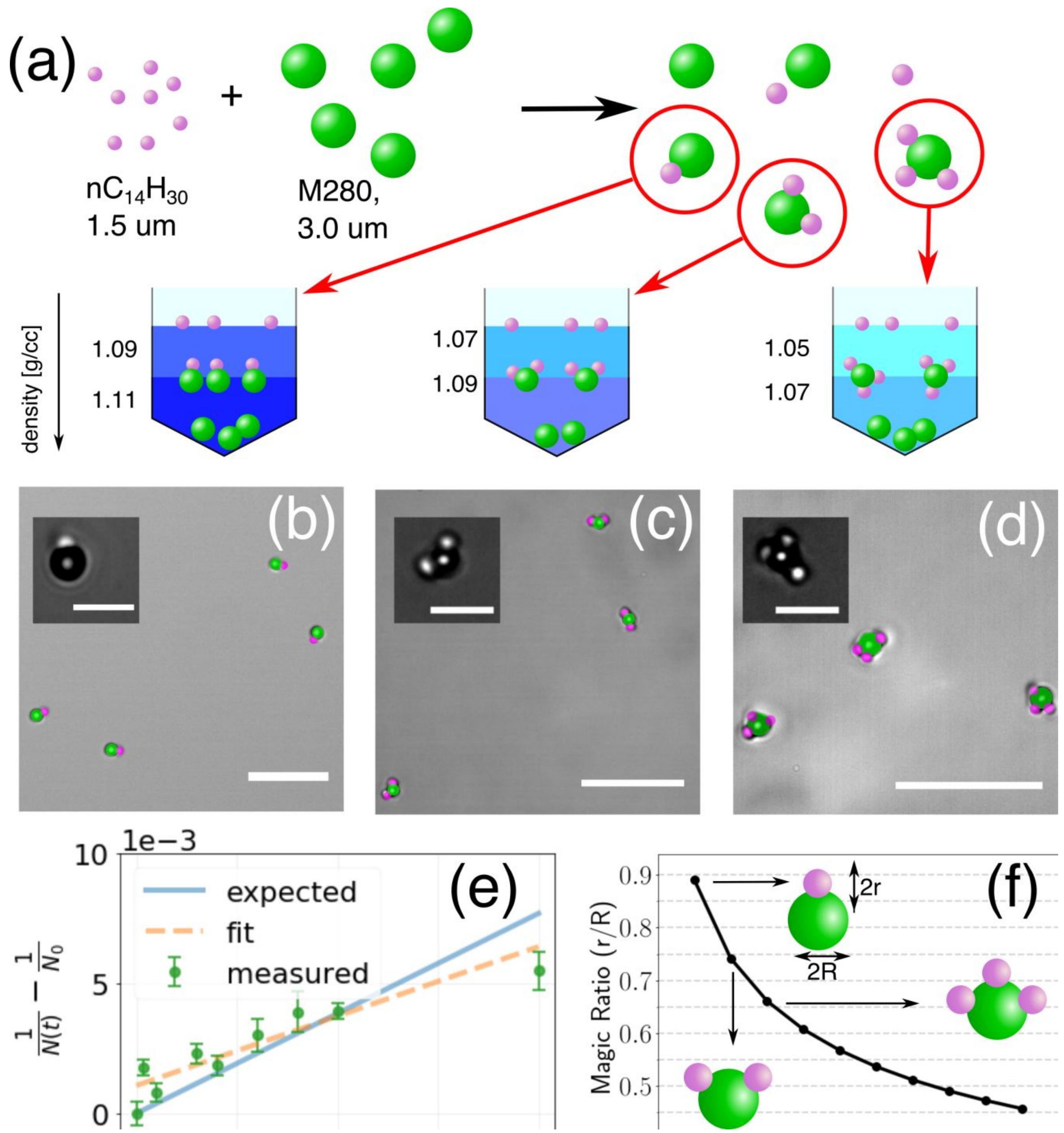

Figure 2. Dimers, trimers, and tetramers synthesis using the mix-and-match strategy. a) By adjusting the density-gradient step it is possible to separately produce: b) dimers, c) trimers and d) tetramers, of a central magnetic particle surrounded by 1.5 µm n-Tetradecane particles (particles are colored for clarity). e) Monitoring the reaction rate between 3 µm magnetic beads and 3 µm n-Decane droplets is quantitatively predicted by a diffusion limited reaction. f) There is a 'magic ratio' between the radii of satellite particles *r* and central particle *R* for optimal

separation of clusters with N satellite particles. The ratio follows $r/R = 1/\sqrt[6]{N(N+1)}$ (see Equation 4). This ratio is useful when it is desired to control the number of particles in a cluster (valence), rather than their size. scalebars: b-d: 20 µm (insets, 5 µm).

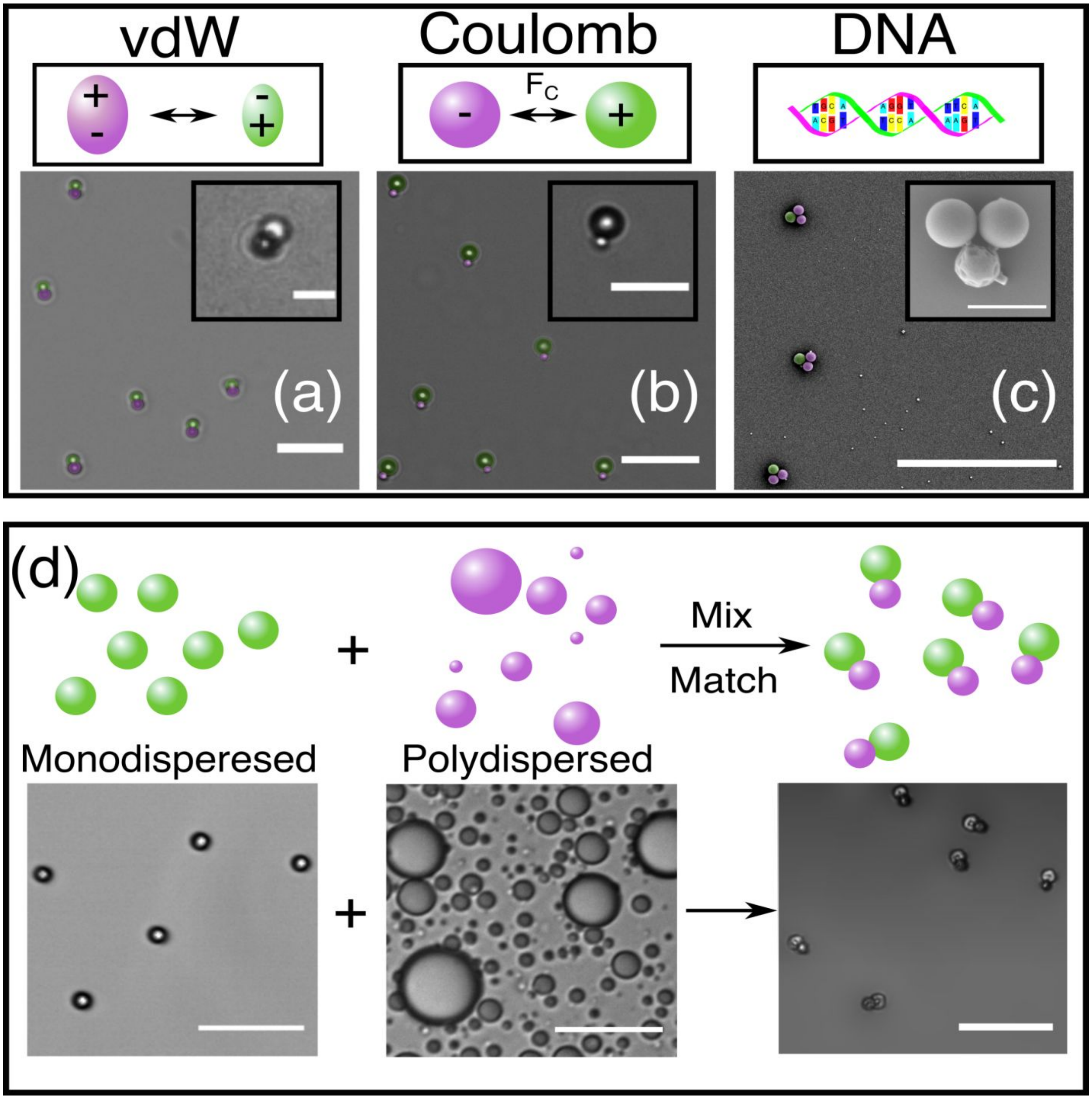

Figure 3. The Mix-and-Match approach applies to a range of particle-particle interactions, with size ranging from sub-micron to a multiple microns (0.6 − 6 μm), and can also produce monodisperse clusters from a highly polydisperse suspension. a) Dimers formed through wetting interaction of 3 μm magnetic particles and 3 μm n-Dodecane droplets. b) Dimers formed by binding 1.86 μm glass particles with 4.2 μm plastic particles through Coulomb attraction. c) Formation of a trimer made of one 0.71 μm PMMA particle and two 0.69 μm PS particles, using

DNA origami functionalized colloids.[39] Inset shows a scanning electron microscope image where the central PMMA particle degrades after exposure to the electron radiation. d) The Mix-and-Match approach can also be used to purify a highly polydisperese emulsion using a monodisperse precursor. Starting with a highly polydispere n-Tetradecane oil emulsion (droplets' size ranging between 0.4 − 400 µm), we use commercially available magnetic beads (3 µm) as the precursor. The resulting suspension consists of dimers made of magnetic particles attached to oil droplets with the droplets diameter range narrowed down to 3−3.3 µm. scalebars: a: 20µm (inset 5 µm), b: 20 µm (inset 2 µm), c: 10 µm (inset, 1 µm), d: 20 µm.

Table 1. Purity yield and throughput comparison for different colloidal interactions

Interaction	Construct	Materials	Density [g/cc]	Purity	Yield	Throughput [10^6 particles/min/mL]
vdW	Dimer	M280, n-Dodecane	1.07	80%	11%	0.8
Coulomb	Dimer	Silica, PS	1.13	96%	10%	9.0
DNA	Trimer	PMMA, PS	1.09	65%	5%	0.4

ASSOCIATED CONTENT

Optical miscroscopy video illustrating the orientation distribution of the asymmetric dimers. (AVI)

Supporting figures showing membrane emulsification product and schematics of hybrid dimer mass distribution. (PDF)

AUTHOR INFORMATION

Corresponding Author

*E-mail: matanbz@gmail.com

Present Addresses

‡ UMR Gulliver 7083 CNRS, ESPCI Paris, PSL Research University, 10 rue Vauquelin, 75005 Paris, France

Author Contributions

The manuscript was written through contributions of all authors. All authors have given approval to the final version of the manuscript.

Conflicts of Interest

There are no conflicts of interest to declare

ACKNOWLEDGMENT

We acknowledge N. Oppenheimer and I. Kolvin for critical reading of the manuscript. This research was primarily supported by the Center for Bio-Inspired Energy Sciences, an Energy Frontier Research Center funded by the DOE, Office of Sciences, Basic Energy Sciences, under award no. DE-SC0000989 (P.M.C.) (M.Y.B.Z.); and grant GBMF3849 from the Gordon and Betty Moore Foundation (P.M.C.) used for DNA design (R.S.). Partial support was provided by U.S. Department of Energy (DOE) under grant DE-SC0007991 (P.M.C.) used for DNA origami design and data analysis. partial support from CHE-1708776 and CCF-1526650 (N.C.S.) for laboratory supplies (R.S.) from the NSF, Grant RGP0010/2017 from the Human Frontiers Science Program, Multidisciplinary University Research Initiative (MURI) W911NF-11-1-0024 from the Army Research Office (N.C.S.) for partial salary support (R.S.), MURI N000141912506 from the Office of Naval Research (N.C.S.) for partial salary support (R.S.), and the Diversity Undergraduate Research Initiative (DURI) New York University for equipment and salary support (Y.C.).

ABBREVIATIONS

PMMA, Poly(methyl methacrylate); PS, polystyrene.

REFERENCES

[1] V. N. Manoharan, M. T. Elsesser, D. J. Pine. Dense Packing and Symmetry in Small Clusters of Microspheres. *Science* **2003**, 301, 5632.

[2] Y. Wang, I. C. Jenkins, J. T. McGinley, T. Sinno, J. C. Crocker. Colloidal crystals with diamond symmetry at optical lengthscales. *Nat. Commun.* **2017**, 8.

[3] Y. Wang, X. Zheng, É. Ducrot, M.-g. G. Lee, G.-r. R. Yi, M. Weck, D. J. Pine. Synthetic Strategies Toward DNA-Coated Colloids that Crystallize. *J. Am. Chem. Soc.* **2015**, 137, 33.

[4] S. Sacanna, W. T. M. Irvine, P. M. Chaikin, D. J. Pine. Lock and key colloids. *Nature* **2010**, 464, 7288.

[5] Y. Wang, Y. Wang, D. R. Breed, V. N. Manoharan, L. Feng, A. D. Hollingsworth, M. Weck, D. J. Pine. Colloids with valence and specific directional bonding. *Nature* **2012**, 491, 7422.

[6] M. E. Leunissen, C. G. Christova, A. P. Hynninen, C. P. Royall, A. I. Campbell, A. Imhof, M. Dijkstra, R. Van Roij, A. Van Blaaderen. Ionic colloidal crystals of oppositely charged particles. *Nature* **2005**, 437, 7056.

[7] D. J. Kraft, R. Ni, F. Smallenburg, M. Hermes, K. Yoon, D. A. Weitz, A. van Blaaderen, J. Groenewold, M. Dijkstra, W. K. Kegel. Surface roughness directed self-assembly of patchy particles into colloidal micelles. *Proc. Natl. Acad. Sci.* USA. **2012**, 109, 27.

[8] L. Feng, L. L. Pontani, R. Dreyfus, P. Chaikin, J. Brujic. Specificity, flexibility and valence of DNA bonds guide emulsion architecture. *Soft Matter* **2013**, 9, 41.

[9] J. D. Forster, J. G. Park, M. Mittal, H. Noh, C. F. Schreck, C. S. O'Hern, H. Cao, E. M. Furst, E. R. Dufresne. Assembly of optical-scale dumbbells into dense photonic crystals. *ACS Nano* **2011**, 5, 8.

[10] A. Fernández-Nieves, G. Cristobal, V. Garcés-Chávez, G. C. Spalding, K. Dholakia, D. A. Weitz. Optically anisotropic colloids of controllable shape. *Adv. Mater.* **2005**, 17, 6.

[11] J. H. Lee, K. J. Gibson, G. Chen, Y. Weizmann. Bipyramid-templated synthesis of monodisperse anisotropic gold nanocrystals. *Nat. Commun.* **2015**, 6, 7571.

[12] N. C. Seeman, *Structural DNA Nanotechnology*. Cambridge University Press, Cambridge, UK **2015**.

[13] M. R. Jones, R. J. Macfarlane, B. Lee, J. Zhang, K. L. Young, A. J. Senesi, C. A. Mirkin. DNA-nanoparticle superlattices formed from anisotropic building blocks. *Nat. Mater.* **2010**, 9, 11.

[14] S. C. Glotzer. Some Assembly Required. *Science* **2004**, 306, 5695.

[15] W. B. Rogers, W. M. Shih, V. N. Manoharan. Using DNA to program the self-assembly of colloidal nanoparticles and microparticles. *Nat. Rev. Mater.* **2016**, 1, 3.

[16] D. R. Nelson. Toward a Tetravalent Chemistry of Colloids. *Nano Lett*. **2002**, 2, 10.

[17] A. P. Alivisatos, K. P. Johnsson, X. Peng, T. E. Wilson, C. J. Loweth, M. P. Bruchez, P. G. Schultz. Organization of 'nanocrystal molecules' using DNA. *Nature* **1996**, 382, 6592.

[18] Z. Gong, T. Hueckel, G.-r. Yi, S. Sacanna. Patchy particles made by colloidal fusion. *Nature* 2017, 550, 7675.

[19] J. M. Romo-Herrera, R. A. Alvarez-Puebla, L. M. Liz-Marzán. Controlled assembly of plasmonic colloidal nanoparticle clusters. *Nanoscale* **2011**, 3, 4.

[20] J. J. D. Joannopoulos, S. Johnson, J. N. J. Winn, R. R. D. Meade, *Photonic Crystals: Molding the Flow of Light*. Princeton University Press, New Jersey, USA **2008**.

[21] K. I. Morozov, A. Leshansky. Photonics of template-mediated lattices of colloidal clusters. *Langmuir* **2019**, 35, 11.

[22] O. Leseur, R. Pierrat, R. Carminati. High-density hyperuniform materials can be transparent. *optica* **2016**, 3, 7.

[23] T. Qiu, T.C. Lee, A. G. Mark, K. I. Morozov, R. Mu, O. Mierka, S. Turek, A. M. Leshansky, P. Fischer, R. Münster, O. Mierka, S. Turek, A. M. Leshansky, P. Fischer. Swimming by reciprocal motion at low Reynolds number. *Nat. Commun.* **2014**, 5 5119.

[24] B. S. Pattni, V. P. Torchilin, in *Targeted Drug Delivery: Concepts and Design,* part I (Eds: Devaraja, Padma V. Jain, Sanyog), Heidelberg, New York, Dordrecht, London **2014**, pp. 3-38.

[25] T. Svedberg, R. Fahraeus. A New Method for the Determination of the Molecular Weight of the Proteins. *J. Am. Chem. Soc.* **1926**, 48, 430.

[26] M. R. Green, J. Sambrook. *"Molecular cloning" A Laboratory Manual*, 4th ed, vol 2. Cold Spring Harbor Press, New York, USA, **2012**.

[27] H. K. Schachman. *Ultracentrifugation in biochemistry*. Academic Press, London, UK, **2013**.

[28] A. D. Edelstein, M. A. Tsuchida, N. Amodaj, H. Pinkard, R. D. Vale, N. Stuurman. Advanced methods of microscope control using u-Manager software. *Journal of Biological Methods* **2014**, 1, 2.

[29] G. Chen, Y. Wang, L.H. Tan, M.Yang, L. H. Tan, Y. Chen, H. Chen. High-Purity Separation of Gold Nanoparticle Dimers and Trimers. *J. Am. Chem. Soc.* **2009**, 131, 12.

[30] J. R. Wolters, G. Avvisati, F. Hagemans, T. Vissers, D. J. Kraft, M. Dijkstra, W. K. Kegel. Self-assembly of "Mickey Mouse" shaped colloids into tube-like structures: experiments and simulations. *Soft Matter* **2015**, 11, 6.

[31] L. Feng, R. Dreyfus, R. Sha, N. C. Seeman, P. M. Chaikin. DNA patchy particles. *Adv. Mater.* **2013**, 25, 20.

[32] Y. Zhang, X. He, R. Zhuo, R. Sha, J. Brujic, N. C. Seeman, P. M. Chaikin. Multivalent, multiflavored droplets by design. *Proc. Natl. Acad. Sci.* USA. **2018**, 115, 37.

[33] A. McMullen, M. Holmes-Cerfon, F. Sciortino, A. Y. Grosberg, J. Brujic. Freely Jointed Polymers Made of Droplets. *Phys. Rev. Lett.* **2018**, 121, 13.

[34] Z. Zeravcic, V. N. Manoharan, M. P. Brenner. Size limits of self-assembled colloidal structures made using specific interactions. *Proc. Natl. Acad. Sci. USA* **2014**, 111, 45.

[35] Z. Zhang, S. C. Glotzer. Self-Assembly of Patchy Particles. *Nano Lett.* **2004**, 4, 8.

[36] M. Doi. *Soft Matter Physics*. Oxford University Press, Oxford, UK **2013**.

[37] P.-G. de Gennes, F. Brochard-Wyart, D. Quere. *Capillarity and Wetting Phenomena*. Springer, Paris, France **2002**.

[38] C. A. Mirkin, R. L. Letsinger, R. C. Mucic, J. J. Storhoff. A DNA-based method for rationally assembling nanoparticles into macroscopic materials. *Nature* **1996**, 382, 6592.

[39] M. Y. Ben Zion, X. He, C. C. Maass, R. Sha, N. C. Seeman, P. M. Chaikin. Self-assembled three-dimensional chiral colloidal architecture. *Science* **2017**, 358, November 633.

[40] J. K. Gansel, M. Thiel, M. S. Rill, M. Decker, K. Bade, V. Saile, G. von Freymann, S. Linden, M. Wegener. Gold helix photonic metamaterial as broadband circular polarizer. *Science* **2009**, 325, 5947.

[41] A. Kuzyk, R. Schreiber, Z. Fan, G. Pardatscher, E.-M. Roller, A. Hogele, F. C. Simmel,

A. O. Govorov, T. Liedl. DNA-based self-assembly of chiral plasmonic nanostructures with tailored optical response. *Nature* **2012**, 483, 7389.

[42] A. Kuzyk, R. Schreiber, H. Zhang, A. O. Govorov, T. Liedl, N. Liu. Reconfigurable 3D plasmonic metamolecules. *Nat. Mater.* **2014**, 13, 9.

[43] R. Schreiber, J. Do, E.-m. Roller, T. Zhang, V. J. Schu, P. C. Nickels, J. Feldmann, T. Liedl. Hierarchical assembly of metal nanoparticles, quantum dots and organic dyes using DNA origami scaffolds. *Nat. Nanotechnol.* **2014**, 9, 1.

[44] M. V. Smoluchowski. Drei Vortrage uber Diffusion, Brownsche Bewegung und Koagulation von Kolloidteilchen. *Physik. Zeitcher.* **1916**, 17, 557-585.

[45] G.R. Yi, T. Thorsen, V. N. Manoharan, M.-j. Hwang, S.-j. Jeon, D. J. Pine, S. R. Quake,

S. M. Yang. Generation of Uniform Colloidal Assemblies in Soft Microfluidic Devices. *Adv. Mater.* **2003**, 15, 15.

BRIEFS (Word Style “BH_Briefs”). If you are submitting your paper to a journal that requires a brief, provide a one-sentence synopsis for inclusion in the Table of Contents.

SYNOPSIS (Word Style “SN_Synopsis_TOC”). If you are submitting your paper to a journal that requires a synopsis, see the journal’s Instructions for Authors for details.